HHS Public Access

Author manuscript

Nanomedicine. Author manuscript; available in PMC 2015 July 01.

Published in final edited form as:

Nanomedicine. 2014 July ; 10(5): 1053–1063. doi:10.1016/j.nano.2013.12.002.

Theranostic tumor homing nanocarriers for the treatment of lung cancer

Apurva R Patel[1], **Mahavir B. Chougule**[2], **Ed Lim**[3], **Kevin P Francis**[3], **Stephen Safe**[4], and **Mandip Singh**[1,*]

[1]College of Pharmacy and Pharmaceutical Sciences, Florida A&M University, Tallahassee, FL 32307

[2]Department of Pharmaceutical Sciences, College of Pharmacy, University of Hawai'i at Hilo, Hilo, HI 96720

[3]Calipers-Life Sciences & Technology - A Perkin Elmer Company, Alameda, CA 94501

[4]Institute of Biosciences and Technology, Texas A&M University, Houston, TX 77030

Abstract

The drugs/strategies to selectively inhibit tumor blood supply has generated interest in recent years for enhancement of cancer therapeutics. The objective of this study was to formulate tumor homing PEGylated CREKA peptide conjugated theranostic nanoparticles of DIM-C-pPhC6H5 (DIM-P) and investigate in vivo antitumor activity as well as evaluate the targeted efficiency to lung tumors using imaging techniques. DIM-P loaded Nanoparticles (NCs-D) were prepared using lipids, and DOGS-NTA-Ni and the surface of NCs-D was modified with PEGylated CREKA peptide (PCNCs-D). PCNCs-D showed 3 fold higher binding to clotted plasma proteins in tumor vasculature compared to NCs-D. PCNCs-D showed 26±4% and 22±5% increase in tumor reduction compare to NCs-D in metastatic and orthotopic models respectively. In-vivo imaging studies showed ~40 folds higher migration of PCNCs-Di in tumor vasculature than NCs-Di. Our studies demonstrate the role of PCNCs-D as theranostic tumor homing drug delivery and imaging systems for lung cancer diagnosis and treatment.

Keywords

Targeted Delivery; Theranostic; Nanoparticles; Tumor homing; Cancer Treatment; In-Vivo Imaging

[*]**Corresponding Author:** Mandip Sachdeva, College of Pharmacy and Pharmaceutical Sciences, Florida A&M University, Tallahassee, FL 32307. Tel: (850) 561-2790; Fax: (850) 599-3318. mandip.sachdeva@famu.edu.

Introduction

Lung cancer is the leading cause of cancer death (28% of all cancer deaths) in both men and women in the United States [1]. Despite recent advances in lung cancer management including chemotherapy, the survival rates in lung cancer patients are unsatisfactory with five-year survival rate of 16.3%, which is lower than other type of cancer such as colon, breast and prostate [1–2]. Currently, newer approaches in the treatment of lung cancer with novel antiangiogenic drugs have generated clinical interest [3]. The vascular endothelial growth factor (VEGF) over-expression (61% to 92% of NSCLC) is associated with poor survival among lung cancer patients [4–5]. Among newer approaches, the use of antiangiogenic agents in combination with other anticancer drugs has generated clinical interest that selectively inhibits the tumor blood supply thus controlling cancer cell survival, proliferation and/or metastasis [6]. Previous studies demonstrated that DIM-C-pPhC6H5 (DIM-P), a c-substituted diindolylmethanes has promising anticancer activity against lung cancer and in combination with Docetaxel showed additive to synergistic action by activating growth inhibitory and apoptotic pathways in lung tumors [7]. Studies conducted in our laboratory strongly suggest that DIM-P exhibits antiangiogenic activity which is evident from down regulation of VEGF and CD31 expression and, decrease in the microvessel density [8]. This warrants further investigations into the antiangiogenic role of DIM-P in the management of lung cancer; however, the pharmacokinetic (PK) studies conducted in our laboratory showed that DIM-P has poor oral bioavailability [9] as well as short plasma half-life following intravenous administration. To overcome this, we used nanoparticle system to deliver DIM-P. Early clinical results have suggested that nanoparticles can enhance efficacy and reduce side effects of therapeutic agents compared to conventional delivery systems [10–11]. However, the outcomes of these passively targeted nanoparticles are hampered due to inefficient tumor cell internalization and toxicity to the normal cells [12–13]. Solid lipid nanoparticles (SLN) have several advantages as compared to other nanoparticles in terms of enhanced stability and alteration of biodistribution [14–16]. However, the use of SLN is limited due to a) low drug loading, and b) drug expulsion thereby decreasing stability. The nanostructured lipid carriers (NCs) have been developed as the second generation lipid nanoparticles [17–18] to overcome barriers of SLN. The higher drug loading capacity and minimal expulsion during storage could be achieved by the development of NCs due to higher solubility of drugs in oils than in solid lipids [19]. The NCs have been utilized to deliver various chemotherapeutic agents [20] and the outer lipid core of the NCs is flexible which allows surface modification with specific groups like PEG-DSPE or DOGS-NTA-Ni which can be utilized for design of multi-targeted delivery systems.

Multifunctional nanoparticles have tremendous potential to improve the clinical outcome of cancer therapeutics as evident from published reports by several researchers [21–23]. One of the tumor homing five amino acid peptides, CREKA (Cys-Arg-Glu-Lys-Ala) was identified using in vivo phage display in MMTV-PyMT transgenic mice [24]. CREKA binds to clotted plasma proteins and homes to the interstitial tissue of tumors and vessel walls containing clotted plasma proteins, whereas normal blood vessels lacks these proteins [24–25]. The selective homing of CREKA peptide to tumor blood vessels and stroma is a novel way to enhance targeting efficacy to tumor blood vasculature. CREKA peptide coupled on the

surface of super-paramagnetic amino dextran-coated iron oxide nanoparticles showed effective anticancer effect in vitro as well as in vivo conditions in breast cancer [26]. Further, CREKA peptide conjugated to Abraxane, a clinically approved paclitaxel-albumin nanoparticle, also showed promising accumulation of CREKA-abraxane in breast tumor blood vessels [27].

The conjugation of polythethylene glycol (PEG) to drug delivery systems has been well reported to increase the half-life and overcome the clearance by the reticuloendothelial system [28–29]. DIM-P showed a short plasma half-life and promising anti-angiogenic activity in lung cancer. Therefore, a delivery approach using PEGylated NCs coupled with targeting to clotted proteins on tumor vasculature using a well studied peptide, CREKA, will overcome limitations associated with delivery of DIM-P and will help to explore its anti-angiogenic potential in the treatment of lung cancer. The proposed mechanistic function of targeted NCs is graphically elaborated in Figure 1. Thus we hypothesize that “Tumor homing PEGylated nanolipidcarriers of DIM-P will target tumor blood vasculature and increase its plasma half life thereby inhibiting tumor growth by exerting antiangiogenic activity against lung tumors”. The specific objectives of this study are: 1) to formulate tumor homing PEGylated CREKA peptide conjugated nanoparticles of DIM-P (PCNCs-D), in conjunction with versions that contain XenolightDiR (PCNCs-Di), 2) to investigate antitumor activity and antiangiogenic potential of PCNCs-D in orthotopic and metastatic lung tumor models, and 3) to evaluate the in-vivo imaging of tumor progression / vasculature and tracking of the nanoparticle using PCNCs-Di. This is the first study to demonstrate delivery of a novel anticancer agent, DIM-P in a pegylated nanocarrier system using CREKA peptide in lung cancer models (orthotopic and metastatic) and demonstrates the application of theranostic nanocarriers in lung tumors. The results from these studies will give researchers critical and important formation for benefits of peptide targeted theranostic nanoparticles in imaging and treatment of lung tumors.

Materials and Methods

Materials and Animals

Further information are given in the Supplementary Data. All animal experimental procedures were done according to the animal experimental ethics committee from our university.

Preparation and Optimization of NCs

NCs were prepared by modified hot melt homogenization technique[30] using triglycerides and optimized process variables. The three formulation variables such as lipid (3, 6, 9 %w/w), peptide/DOGS-NTA-Ni ratio and PEG molecular weight were varied at three concentration levels to achieve desired efficiency.

Freeze Drying of NCs

Formulations were lyophilized (SMART Freeze Drying, FTS Systems, SP Scientific, USA) using a universal stepwise freeze drying cycle. Formulations were lyophilized using 5% w/v

trehalose (cryoprotectant) and the viscosity of the NCs formulations was adjusted to 2.5-3cP by re-suspending the lyophilized formulation in distilled water prior to use.

Preparation and Optimization of PCNCs

For surface modification, 200 μl of NCs were mixed with 50 μl of 6-Histidine -tagged PEGylated (PEG-2000) CREKA peptide aqueous solution (5 mg/ml) and incubated for 2 hr at room temperature with constant stirring.

Characterization of NCs & PCNCs

Particle Size, Zeta Potential, Entrapment Efficiency and Drug loading Measurement—The particle size and zeta potential of NCs or PCNCs were measured in distilled water using Nicomp 380 ZLS (Particle Sizing Systems, Port Richey, FL) as described previously[30]. Entrapment efficiency was determined as reported earlier using vivaspin columns, molecular weight cut-off (MWCO) 10,000 Da [30].

In-vitro drug release studies—In-vitro drug release studies were conducted with a cellulose membrane using a USP Type-I dissolution apparatus (Vankel, NC) for 72 h with the help of 200 ml of phosphate buffer saline (PBS) pH 7.4 containing 0.5% w/v Volpo-20 & 0.5% TPGS as dissolution medium. The in-vitro drug release of DIM-P solution, NCs-D and PCNCs-D were carried out as described in supplementary data.

Differential Scanning Calorimetry—The interaction of DIM-P with lipids and association of DIM-P in NCs formulations were determined using a DSCQ100 (TA instrument, DE).

Accelerated stability studies—Freeze-dry NCs-D were stored at different temperatures 30±1°C, 40±1°C and 50±1°C; and also at room temperature (mean temperature being 25.7 ± 0.6°C) for three month [31]. Aliquots were removed after intervals of time (0, 15, 30, 60 and 90 days) for stability analysis.

In-vitro analysis of NCs-D and PCNCs-D

Clot Binding Assay—Efficacy of NCs & PCNCs to bind clotted plasma was evaluated using clot binding assay as described in supplementary data. The clot binding assay was used to optimize the concentration of CREKA peptide to that of the DOGS-Ni-NTA.

In-vitro cytotoxicity—In-vitro cytotoxicity of PCNCs-D formulation was carried out in H460 and HUVEC cell lines [30].

Tube formation assay—Tube formation assay was performed using Endothelial Cell Tube Formation Assay Kit (Invitrogen Life Technologies™ , USA).

In-vivo analysis of NCs-D and PCNCs-D

Pharmacokinetic Analysis of NCs-D and PCNCs-D—Pharmacokinetic properties of DIM-P in BALB/c mice were determined following I.V. administration of NCs-D & PCNCs-D (DIM-P equivalent to 5.0 mg/kg.

Evaluation of anti-angiogenic efficacy—Geltrex™ (Invitrogen Life Technologies™ , USA) was used for the gel plug assay to evaluate anti-angiogenic effect of DIM-P, NCs-D and PCNCs-D.

In-vivo anticancer evaluation in lung cancer models

Tumor bearing mice were randomly divided into the following each group (n=10) to receive various DIM-P formulations; A) control group received vehicle (placebo NCs); B) NCs-D (DIM-P equivalent of 0.5 mg/kg) every third day C) PCNCs-D (DIM-P equivalent of 0.5 mg/kg) every third day D) DIM-P solution (0.5 mg/kg) every third day. The lung weights and tumor volume were used for assessment of the therapeutic activity of the treatments. Tumor tissue were removed and analyzed for different protein markers by Immunohistochemistry and Western Blotting.

In-vivo imaging of tumors and tracking of NCs & PCNCs

Optical Imaging—Following the injection of NC-Di and PCNC-Di, fluorescent imaging of whole body and tumor area of animals were done at different time points. Targeting to the tumor vasculature by NCs-Di and PCNCs-Di was quantified by drawing a region of interest (ROI) around the tumor area and measuring fluorescence as total radiant efficiency, [p/s] / [μW/cm^2].

Ultrasound Imaging—Ultrasound imaging was performed using a Vevo2100 from VisualSonics, Inc. Tumor images were analyzed using VisualSonics imaging software package. For angiogenesis evaluation, VEGFR2 targeted microbubbles in tumor bearing mice were used after treatment with PCNCs and NCs.

Statistical analysis

Pooled data were expressed as mean ± standard deviations (SD) and model parameters as estimates with ± standard errors (SE). Means were compared between two groups by student's *t* test and between three dose groups by one-way variance analysis (ANOVA). Correlations between doses and parameters were sought by use of the linear regression coefficient (r) and the coefficient of determination (R^2). Probability (p) values < 0.05 were considered significant. All statistical analyses were performed using GraphPad Prism® 5.0 software (San Diego, CA).

Results

Characterization of NCs & PCNCs

The optimizes NCs-D formulation prepared using triglycerides had a particle size of 177 ± 20 nm and polydispersity of 0.20 ± 0.05. PCNCs had a particle size of 190 ± 17 nm and polydispersity of 0.21±0.06. The zeta potential of NCs-D and PCNCs-D formulations in distilled water was −27.38 ± 2.98 and −25.30 ± 3.21 mV, respectively. The total DIM-P content assay results indicated that approximately 1.9 mg/ml of DIM-P was present in the NCs formulation. The entrapment efficiency (EE) and drug loading of formulations were 96.2 ± 2.5% and 7.5 ± 1.5% w/w respectively. Furthermore, it was found that ~ 150–200 molecules of CREKA peptide were present on each nanoparticle (PCNCs) surface. The

NCs-D and PCNCs-D formulations were able to release the DIM-P in controlled manner and more than 90% of drug was released after 72 hr (Figure 2A). The DSC thermograms of DIM-P, NCs-D and NCs are represented in Figure S1.

In-vitro analysis of NCs-D and PCNCs-D

Efficacy of NCs was evaluated using clot binding assay as described. PCNCs-D showed significant ($p<0.001$) 3 fold higher binding to the clotted plasma proteins compared to NCs-D and a nonspecific YKA peptide coated NCs (YNCs-D) (Figure 2B). CREKA peptide of 152 μM was found to be optimal for binding to the plasma clot and with higher concentration showed saturation effect (Figure 2B). The DIM-P showed IC_{50} value of 6.8 and 2.1μM against H460 and HUVEC cells respectively. The NCs-D, NCs-D-NTA and PCNC-D showed comparable IC_{50} value to DIM-P with no statistical differences ($p>0.05$) against H460 and HUVEC cells, suggesting that DIM-P was still active when entrapped in PCNCs-D (Table S1). The placebo NCs showed >98% viability of H460 and HUVEC cells demonstrating non-toxicity and safety of excipients used in development of NCs. Anti-angiogenic effects of DIM-P solution, NCs-D and PCNCs-D were analyzed using an in vitro tube-formation assay as described in method section. Briefly, after seeding on Matrigel, HUVEC cells were incubated with DIM-P (10 μM), NCs-D (10 μM) and PCNCs-D (10 μM) for 6 hr. The results show that tube-like structures were poorly organized (Figure 2D-F) and decreased in capillary tube branch point formation with NCs-D, PCNCs-D and DIM-P solution. In contrast, in control group, HUVECs formed a rich meshwork of branching capillary-like tubules with multicentric junctions within 6 hr (Figure 2C). Tube formation assay results showed that the DIM-P and PCNCs-D formulations significantly ($p<0.05$) inhibited tube formation suggesting anti-angiogenic activity of DIM-P.

In-vivo analysis of NCs-D and PCNCs-D

Pharmacokinetic Analysis of NCs-D and PCNCs-D—The plasma pharmacokinetic of DIM-P solution, NCs-D and PCNCs-D following intravenous administration are shown in Figure 3. The plasma drug-concentration profile following i.v. administration of DIM-P solution showed less than 2 h apparent distributional phase followed by prolonged disposition through the sampling times. However, NCs-D and PCNCs-D plasma concentrations declined slowly compared to that of DIM-P. Thus, i.v. administration of DIM-P, NCs-D and PCNCs-D were first investigated as a two compartment model. The two compartment linear model revealed a poor structural fit with the data, suggesting that another kinetic process may be involved for DIM-P. As for NCs-D, two compartment linear model was fitted with the data observed, and PCNCs-D showed a two compartment linear model structural fit with -1α error model. The primary and secondary parameters estimated from curve fitting following i.v. administration of 5 mg/kg are shown in Table S2.

Evaluation of anti-angiogenic efficacy

Matrigel plug assay was carried out in C57BL/6 mice to assess anti-angiogenic effect of NCs-D and PCNCs-D in-vivo. The hemoglobin (Hb) content in plugs was quantified using the Drabkin's reagent kit to measure the anti-angiogenic response. The hemoglobin (Hg) levels in samples were measured by a colorimetric assay. The levels of Hg were compared

with normal adjacent tissues. The metrigel plug Hg content served as an indicator of vascularization. An decrease in the Hg content in metrigel plug with the treatment with NCs-D and PCNCs-D compared with the control was observed (Table S3).

In vivo anticancer evaluation in lung cancer models

The anticancer activity of DIM-P as NCs-D & PCNCs-D was investigated in female athymic nude mice bearing A549 orthotopic and H1650 metastatic lung tumors. Treatment was started ten days after tumor implantation and continued for a total of 35 days. The results (Figure 4A) show that lung tumor weights were significantly (*, $p<0.001$) decreased after treatment with NCs-D and PCNCs-D compared to control. Lung tumor weight reduction of 20 and 47 % was observed in mice treated with NCs-D and PCNCs-D respectively. Lung tumor volume reduction (Figure 4B) in mice treated with NCs-D and PCNCs-D were 31 and 53 % respectively. A non-significant ($p>0.05$) change in average number of tumor nodules was observed among central, mid and peripheral regions of harvested lungs from each treated groups. NCs-D and PCNCs-D treatment showed a significant (*, $p<0.001$) decrease in average number of tumor nodules in central, mid and peripheral regions compared to control groups. We did not observe any weight loss or other signs of toxicity in mice treated with NCs-D or PCNCs-D (Figure 4C). Also, the anticancer activity of DIM-P as NCs-D & PCNCs-D in female athymic nude mice bearing H1650 metastatic lung tumors showed similar results (Figure 4D-F).

Immunohistochemistry (VEGF & CD31 expression) and Western blot analysis

To examine if the NCs-D & PCNCs-D inhibited lung tumor growth through inhibition of angiogenesis and to confirm our preliminary result of antiangiogenic activity of DIM-P, we determined VEGF expression in tumor tissue sections by IHC. A significant (*p <0.05) decreased expression of VEGF (Figure 5A) was observed in tumors treated with the NCs-D & PCNCs-D treatment compared to untreated group. CD31 (+) endothelial cells were also identified, as illustrated in Figure 5B. The staining of microvessels in NCs-D & PCNCs-D treated groups was significant (*p <0.05) decreased compared to control group. The average number of microvessels per field in groups treated with NCs-D & PCNCs-D were found to be 99 ± 6.6 (*,$p<0.05$), 52 ± 10.5 (**,$p<0.001$) respectively compared to 179.0 ± 28.4 in the control group. The analysis of proliferation marker Ki-67 (Figure S2) indicates the inhibition (*p <0.05) of lung tumors progression in NCs-D and PCNCs-D treated groups of animals. The average number of proliferative Ki-67 positive cells per field in groups treated with NCs-D & PCNCs-D were found to be 86 ± 9 (*,p<0.05), 41 ± 11 (**,p<0.001) respectively compared to 158.0 ± 22.0 in the control group. We compared expression of several proteins in normal lung tissue lysates, tumor lysates from control and treated mice by Western blot analysis using β-actin as loading control (Figure 5C). NCs-D & PCNCs-D treatment significantly (*p<0.05) decreased MMP-9 expression to 0.26 and 0.54-fold in regressed tumor samples compared to controls groups respectively. In regressed tumors, the PCNCs-D (*, p<0.001) and NCs-D (*, p<0.01) significantly decreased HIF-1α expression to 0.48, and 0.15-fold, respectively of the controls (Figure 5C). PCNCs-D treatment showed increased Erk2 protein expression (**, p<0.05) to 0.67-fold compared to 0.28-fold NCs-D (*, p<0.01) respectively of the controls in regressed tumors (Figure 5C). The NCs-D & PCNCs-D decreased Sp1 expression significantly (*, p<0.001) compared to tumors harvested from

control group (Figure 5C). PCNCs-D & NCs-D treatment significantly (*, $p<0.05$) decreased Sp3 expression to 0.29 and 0.09-fold respectively in regressed tumor samples compared to control groups (Figure 5C). The expression of HSP-27 protein were significantly decreased by 0.13 fold (*, $p<0.01$) and 0.44 fold (*, $p<0.05$) with PCNCs-D & NCs-D treatment compared to control group respectively (Figure 5C). Results illustrated in Figure 5C show that the PCNCs-D treatment significantly decreased expression of VEGF to 0.6- fold (*, $p<0.001$) compared to control.

In-vivo imaging of tumors and tracking of NCs & PCNCs

In-vivo imaging following exposure of PCNCs-Di demonstrated their targeting to the tumor vasculature (Figure 6), where the PCNCs-Di were found to migrate more in newly formed blood vessels with total radiant efficiency [p/s] / [μW/cm^2] of $2.1*10^{12} \pm 0.5*10^{12}$ over the period of 0.5 hr to 3h. NCs-Di didn't show any specific migration to tumors confirming the specific targeting of PCNCs-Di with total radiant efficiency [p/s] / [μW/cm^2] of $0.6*10^{11} \pm 0.18*10^{11}$. Also, nanoparticle distribution analysis showed that NCs-Di were not uniformly distributed throughout the body and migrated to organs such as liver, lung etc. On the contrary, PCNCs-Di showed uniform distribution of nanoparticles and did show more migration to tumor region compared to other organs in the body (Figure S3). Furthermore, targeting efficiency and delivery of entrap material by NCs-D and PCNCs-D was confirmed using luciferase reporter (bioluminescence in-vivo imaging) system (Figure S4)

The particles conjugated to ligands targeting VEGFR2 were utilized and the Vevo system was able to quantify angiogenesis relative to the tumor. There was a significant ($p<0.05$) decrease in contrast enhancement in mice treated with PCNCs-D and NCs-D compared with the control-treated group (Figure 6). Relative contrast mean intensity values [linear arbitrary units (a.u.)] for animals treated with PCNCs (3.9 ± 1.5) were significantly ($p<0.01$) decreased than in control-treated animals (19.8 ± 1.1) and NCs-D treated animals (12.5 ± 1.4) ($p<0.05$). Furthermore, we analyzed the vascular blood flow/perfusion kinetics of tumor and surrounding tissue (Figure S5). Similar to in-vivo angiogenesis assay, we found decrease in tumor blood flow with treatment of PCNCs-Di compared to NCs-Di and control. The relative contrast mean intensity values [linear arbitrary units (a.u.)] for bolus perfusion/ blood flow kinetics in animals treated with PCNCs (8.93 ± 1.90) were significantly ($p<0.01$) decreased than in control-treated animals (57.83 ± 16.89) and NCs-D treated animals (40.85 ± 1.69) in orthotopic tumors, whereas non-tumor bearing mice showed intensity values of 2.6 ± 1.65.

Discussion

In this study, we have developed a novel theranostic approach for treatment and imaging of lung cancer using targeted multifunctional PCNCs. The triglycerides such as compritol, monosterol, precirol and miglyol were used to prepare the NCs formulations. The NCs are flexible which allows surface modification with specific groups like PEG-DSPE or DOGS-NTA-Ni and useful for design of multi-targeted delivery systems. Thus, we have utilized a rational approach in designing stable and multifunctional NCs and evaluated its efficacy against lung cancer.

The approach of using DOGS-NTA-Ni spacer for linking to histidine tagged CREKA peptide exploits the interaction between chelated divalent metal ions such as nickel and a short sequence of histidine residues, referred to as histidine-tags (His-tag). Which provides a simple, efficient and reproducible technique to conjugate the His tag PEGylated CREKA peptide onto the NCs surface using metal chelating lipids as spacer. In the present study, we used six histidine groups at the N-terminal end of the CREKA peptide to conjugate on to the NCs surface. We have evaluated DOGS-NTA-Ni toxicity under in vitro conditions due to presence of Ni by exposing normal small airway epithelial cells. Our results showed that DOGS-NTA-Ni (0.1–27% w/v) showed > 97% viability for normal small airway epithelial cells suggesting safety profile of DOGS-NTA-Ni (Figure S6). To prepare PCNCs-D, we have used DOGS-NTA concentration of 0.1–0.3% w/v which is 66 fold lower than the evaluated dose by Chikh et al in vivo [32] and 90 fold lower than highest concentration of our in vitro safety data against normal airway epithelial cells.

Anti-angiogenic approaches have been found to be effective in limiting tumor growth and also have advantages compared to conventional therapies such as (i) overcoming the physiological barrier, (ii) decrease the tumor growth and metastasis; and (iii) diminishing secondarily acquired drug resistance [33–35]. VEGF receptors, αvβ3 integrins, and matrix metalloproteinase receptors are main targets which have been explored using nanoparticle systems against different cancers [13]. Current treatment with FDA approved bevacizumab, an anti-VEGF antibody, is associated with severe cardiovascular side effects [36]. Therefore, newer therapeutic options need to be investigated to improve the clinical outcome of lung cancer. The CREKA peptide binds to clotted plasma proteins and homes to the interstitial tissue of tumors and vessel walls containing clotted plasma proteins, whereas normal blood vessels lacks these proteins [24–25]. Ruoslahti et al [26–27] showed CREKA coated iron oxide nanoparticles and CREKA coated abraxane nanoparticles delivered to tumors bind to the walls of tumor vessels and cause clotting in them. CREKA peptide coated DIM-P nanoparticles also showed an accumulation in tumor vessels as evident from co-localization of the nanoparticles evaluated using in-vivo imaging studies (Figure 6). Our in vivo results showed an effective tumor therapy and imaging strategy that is based on synergistic and self-amplifying accumulation of homing peptide–coated nano-lipid carriers in lung tumor blood vessels.

The NCs showed a desirable size of < 200 nm for targeting lung tumors. Our in-vitro studies confirm the encapsulation and controlled release of DIM-P from NCs-D and PCNCs-D. The release pattern of DIM-P from NCs-D was found to be zero order kinetics. Cytotoxicity analysis showed >98 percent viability of H460 and HUVEC cells with placebo NCs demonstrating non-toxicity and safety of excipients used in the preparation of NCs formulations, while NCs-D treatment confirmed anticancer and antiangiogenic activity of DIM-P. The NCs-D and PCNCs-D formulations were found to be effective in inhibition of NSCLC and HUVEC cells in vitro. Furthermore, the targeted PCNCs-D showed more inhibition of tumors compare to NCs-D.

The efficiency of the PCNCs-D may be correlated with the degree of tumor vessel blockade achieved with treatment. In-vivo angiogenic assay using Geltrex showed that NCs-D treatment induced 27% ($p<0.05$) reduction in Hb content compare to the 72% ($p<0.01$)

reduction in Hb content by PCNCs-D therapy. The reduction in Hb content was in co-relation with increased amount of PCNCs-D at site of action. Similarly, Ruoslahti et al [24] showed that the efficiency of the CREKA nanoworms was strongly correlated with the degree of tumor vessel blockade achieved with the various treatments. Significantly, our results were obtained using only the inherent properties of the nanoparticles, which also allowed imaging of the tumors and further enhanced the utility of this theranostic nanosystem.

To further confirm the fate of PCNCs and NCs, we used whole body imaging using an NIR fluorescent probe (Xenolight DiR) instead of DIM-P. Both NCs-Di and PCNCs-Di circulated fairly uniformly when injected intravenously. There was accumulation of NCs-Di in the liver and lung which may be due to uptake by the RES (opsonization), where certain plasma proteins bind to particulate material to eliminate them from circulation [37]. PCNCs-D prolonged the half-life of DIM-P compared to NCs-D, as shown by pharmacokinetic analysis which was substantiated by imaging of PCNCs-Di in vivo. The PEGylation of PCNCs is most likely responsible for this, since its hydrophilicity, flexibility, and neutral charge in biological fluids helps in their dispersion and increases their blood circulation times [38–40]. PCNCs primarily localized in tumor blood vessels (distinct tumor blood vessel structure is seen in tumor micro-environment, Figure 6). The local concentration of PCNCs-Di was almost 50 fold higher than NCs-Di in terms of radiant efficiency flux. Other organs contained minor, if any amounts of PCNCs (Figure S2). Also, tumor tissue analysis showed about 26.82±6.89% more DIM-P concentration in tumors at 6 hr collected from single treatment with PCNCs-D compare to NCs-D. Also, the perfusion kinetic analysis by ultrasound imaging showed decreased blood flow in the PCNCs-D treatment group compared to NCs-D treated and control groups.

DIM-P and related 1, 1-bis (3’-indolyl)-1-(substituted phenyl) methane compounds inhibit tumor growth and induce apoptosis in lung and other cancer cell lines and the mechanisms of these responses are structure-independent [41–43]. Several researchers have shown the involvement of orphan nuclear receptor involvement in tumor angiogenesis. Huying et.al showed that TR3/Nur77 regulates VEGF induced angiogenesis [44] and Zhao et.al reported the role of Nurr1 in angiogenesis through CREB dependent mechanism [45]. Studies by Wu et.al showed decreased expression of VEGF, MMP-2 and MMP-9 with indole-3-carbinol (I3C) treatment[46]. Also, Chang et.al reported that 3, 3’-diindolylmethane (DIM) was found to inhibit angiogenesis in breast cancer xenograft model in mice [47]. In present investigations, we have evaluated the efficacy of DIM-P and PCNCs-D for down-regulation of expression of angiogenic and proliferative markers such as Ki-67, CD31, VEGF, HIF-α and specificity proteins (Sp). Figure 5 indicates that treatment of DIM-P solution, NCs-D and PCNCs-D significantly decreased expression of angigiogenic markers HSP-27, HIF-α, Sp1 & Sp3 proteins compared to control. Our results demonstrate that the possible underlying molecular targets of DIM-P in NSCLC are inhibition of proliferative marker Ki-67, VEGF, CD 31 and HIF-1α, and targeted degradation of Sp1, and Sp3 proteins involved in angiogenesis as well as decreased expression of MAPK, PLC-γ and Erk2. Similar to our finding, Yamada et. al [48] reported decrease in expression of Ki-67 and CD31 was related to anti-angiogenic activity. DIM-P has been shown to have anti-cancer activity as previously reported but our findings also suggest that it may have anti-angiogenic effect

as well. Also, Jacques et.al reported that DIM treatment decreased the accumulation and activity of the key angiogenesis regulatory factor, HIF-1 alpha, in hypoxic tumor cells [49]. Helen et al. reported possible role of C-DIMs (DIMC-pPhOCH3, DIM-C-pPhOH, DIM-C-pPhCl) in inhibition of angiogenesis through NR4A nuclear orphan receptor[50].

Our in vitro and in vivo results demonstrate that DIM-P inhibits angiogenesis via VEGF and Sp pathways. Our results further suggest that the efficacy of DIM-P was enhanced with use of PCNCs-D compared to non-targeted NCs and drug solution. In addition, our approach of using PCNCs-D for delivery of DIM-P could overcome the PK limitations associated with DIM-P and could be used as a single agent in treatment of lung cancer. Using ultrasound, NIR fluorescent and bioluminescent in vivo imaging, we were able to design and evaluate the drug-carrying nanoparticles that amass in tumor vessels and slowly release their drug payload, while simultaneously occluding the vessels.

Supplementary Material

Refer to Web version on PubMed Central for supplementary material.

Acknowledgments

All sources of support for research

This work was financially supported by National Institute of Health - MBRS-SC1 Program (Grant # SC1 GM092779-01).

References

1. Molina JR, Yang P, Cassivi SD, Schild SE, Adjei AA. Non-small cell lung cancer: epidemiology, risk factors, treatment, and survivorship. Mayo Clin Proc. 2008; 83(5):584–594. [PubMed: 18452692]
2. Siegel R, Naishadham D, Jemal A. Cancer statistics, 2012. CA Cancer J Clin. 2012; 62(1):10–29. [PubMed: 22237781]
3. Schmid-Bindert G. Update on antiangiogenic treatment of advanced non-small cell lung cancer (NSCLC). Target Oncol. 2013
4. Han H, Silverman JF, Santucci TS, Macherey RS, d'Amato TA, Tung MY, Weyant RJ, Landreneau RJ. Vascular endothelial growth factor expression in stage I non-small cell lung cancer correlates with neoangiogenesis and a poor prognosis. Ann Surg Oncol. 2001; 8(1):72–79. [PubMed: 11206229]
5. Fontanini G, Faviana P, Lucchi M, Boldrini L, Mussi A, Camacci T, Mariani MA, Angeletti CA, Basolo F, Pingitore R. A high vascular count and overexpression of vascular endothelial growth factor are associated with unfavourable prognosis in operated small cell lung carcinoma. Br J Cancer. 2002; 86(4):558–563. [PubMed: 11870537]
6. Gasparini G, Longo R, Fanelli M, Teicher BA. Combination of antiangiogenic therapy with other anticancer therapies: results, challenges, and open questions. J Clin Oncol. 2005; 23(6):1295–1311. [PubMed: 15718328]
7. Ichite N, Chougule MB, Jackson T, Fulzele SV, Safe S, Singh M. Enhancement of docetaxel anticancer activity by a novel diindolylmethane compound in human non-small cell lung cancer. Clin Cancer Res. 2009; 15(2):543–552. [PubMed: 19147759]
8. Ichite N, Chougule M, Patel AR, Jackson T, Safe S, Singh M. Inhalation delivery of a novel diindolylmethane derivative for the treatment of lung cancer. Mol Cancer Ther. 2010; 9(11):3003–3014. [PubMed: 20978159]

9. Patel AR, Spencer SD, Chougule MB, Safe S, Singh M. Pharmacokinetic evaluation and in vitro-in vivo correlation (IVIVC) of novel methylene-substituted 3,3' diindolylmethane (DIM). Eur J Pharm Sci. 2012; 46(1-2):8–16. [PubMed: 22342559]
10. Emeje MO, Obidike IC, Akpabio EI, Ofoefule SI. Nanotechnology in Drug Delivery. 2012
11. Cho K, Wang X, Nie S, Chen ZG, Shin DM. Therapeutic nanoparticles for drug delivery in cancer. Clin Cancer Res. 2008; 14(5):1310–1316. [PubMed: 18316549]
12. Sinha R, Kim GJ, Nie S, Shin DM. Nanotechnology in cancer therapeutics: bioconjugated nanoparticles for drug delivery. Mol Cancer Ther. 2006; 5(8):1909–1917. [PubMed: 16928810]
13. Byrne JD, Betancourt T, Brannon-Peppas L. Active targeting schemes for nanoparticle systems in cancer therapeutics. Adv Drug Deliv Rev. 2008; 60(15):1615–1626. [PubMed: 18840489]
14. Kirpotin DB, Drummond DC, Shao Y, Shalaby MR, Hong K, Nielsen UB, Marks JD, Benz CC, Park JW. Antibody targeting of long-circulating lipidic nanoparticles does not increase tumor localization but does increase internalization in animal models. Cancer Res. 2006; 66(13):6732–6740. [PubMed: 16818648]
15. Iinuma H, Maruyama K, Okinaga K, Sasaki K, Sekine T, Ishida O, Ogiwara N, Johkura K, Yonemura Y. Intracellular targeting therapy of cisplatin-encapsulated transferrin-polyethylene glycol liposome on peritoneal dissemination of gastric cancer. Int J Cancer. 2002; 99(1):130–137. [PubMed: 11948504]
16. Wong HL, Bendayan R, Rauth AM, Li Y, Wu XY. Chemotherapy with anticancer drugs encapsulated in solid lipid nanoparticles. Adv Drug Deliv Rev. 2007; 59(6):491–504. [PubMed: 17532091]
17. Souto EB, Wissing SA, Barbosa CM, Muller RH. Development of a controlled release formulation based on SLN and NLC for topical clotrimazole delivery. Int J Pharm. 2004; 278(1):71–77. [PubMed: 15158950]
18. Pardeike J, Hommoss A, Muller RH. Lipid nanoparticles (SLN, NLC) in cosmetic and pharmaceutical dermal products. Int J Pharm. 2009; 366(1-2):170–184. [PubMed: 18992314]
19. Muller RH, Radtke M, Wissing SA. Solid lipid nanoparticles (SLN) and nanostructured lipid carriers (NLC) in cosmetic and dermatological preparations. Adv Drug Deliv Rev. 2002; 54(Suppl 1):S131–S155. [PubMed: 12460720]
20. Selvamuthukumar S, Velmurugan R. Nanostructured Lipid Carriers: A potential drug carrier for cancer chemotherapy. Lipids Health Dis. 2012; 11:159. [PubMed: 23167765]
21. van Vlerken LE, Amiji MM. Multi-functional polymeric nanoparticles for tumour-targeted drug delivery. Expert Opin Drug Deliv. 2006; 3(2):205–216. [PubMed: 16506948]
22. Muthu MS, Kulkarni SA, Raju A, Feng SS. Theranostic liposomes of TPGS coating for targeted co-delivery of docetaxel and quantum dots. Biomaterials. 2012; 33(12):3494–3501. [PubMed: 22306020]
23. Wu W, Shen J, Gai Z, Hong K, Banerjee P, Zhou S. Multi-functional core-shell hybrid nanogels for pH-dependent magnetic manipulation, fluorescent pH-sensing, and drug delivery. Biomaterials. 2011; 32(36):9876–9887. [PubMed: 21944827]
24. Simberg D, Duza T, Park JH, Essler M, Pilch J, Zhang L, Derfus AM, Yang M, Hoffman RM, Bhatia S, Sailor MJ, Ruoslahti E. Biomimetic amplification of nanoparticle homing to tumors. Proc Natl Acad Sci U S A. 2007; 104(3):932–936. [PubMed: 17215365]
25. Dvorak HF, Senger DR, Dvorak AM, Harvey VS, McDonagh J. Regulation of extravascular coagulation by microvascular permeability. Science. 1985; 227(4690):1059–1061. [PubMed: 3975602]
26. Agemy L, Sugahara KN, Kotamraju VR, Gujraty K, Girard OM, Kono Y, Mattrey RF, Park JH, Sailor MJ, Jimenez AI, Cativiela C, Zanuy D, Sayago FJ, Aleman C, Nussinov R, Ruoslahti E. Nanoparticle-induced vascular blockade in human prostate cancer. Blood. 2010; 116(15):2847–2856. [PubMed: 20587786]
27. Karmali PP, Kotamraju VR, Kastantin M, Black M, Missirlis D, Tirrell M, Ruoslahti E. Targeting of albumin-embedded paclitaxel nanoparticles to tumors. Nanomedicine. 2009; 5(1):73–82. [PubMed: 18829396]
28. Jokerst JV, Lobovkina T, Zare RN, Gambhir SS. Nanoparticle PEGylation for imaging and therapy. Nanomedicine (Lond). 2011; 6(4):715–728. [PubMed: 21718180]

29. Stefanick JF, Ashley JD, Kiziltepe T, Bilgicer B. A Systematic Analysis of Peptide Linker Length and Liposomal Polyethylene Glycol Coating on Cellular Uptake of Peptide-Targeted Liposomes. ACS Nano. 2013

30. Patel AR, Chougule MB, I T, Patlolla R, Wang G, Singh M. Efficacy of aerosolized celecoxib encapsulated nanostructured lipid carrier in non-small cell lung cancer in combination with docetaxel. Pharm Res. 2013; 30(5):1435–1446. [PubMed: 23361589]

31. Singh A, Ahmad I, Akhter S, Jain GK, Iqbal Z, Talegaonkar S, Ahmad FJ. Nanocarrier based formulation of Thymoquinone improves oral delivery: Stability assessment, in vitro and in vivo studies. Colloids and Surfaces B: Biointerfaces. 2013; 102(0):822–832.

32. Chikh GG, Li WM, Schutze-Redelmeier MP, Meunier JC, Bally MB. Attaching histidine-tagged peptides and proteins to lipid-based carriers through use of metal-ion-chelating lipids. Biochim Biophys Acta. 2002; 1567(1-2):204–212. [PubMed: 12488054]

33. Folkman J. Fighting cancer by attacking its blood supply. Sci Am. 1996; 275(3):150–154. [PubMed: 8701285]

34. Giaccone G. The potential of antiangiogenic therapy in non-small cell lung cancer. Clin Cancer Res. 2007; 13(7):1961–1970. [PubMed: 17404076]

35. Kumar S, Li C. Targeting of vasculature in cancer and other angiogenic diseases. Trends Immunol. 2001; 22(3):129. [PubMed: 11334027]

36. Ferrara N, Hillan KJ, Novotny W. Bevacizumab (Avastin), a humanized anti-VEGF monoclonal antibody for cancer therapy. Biochem Biophys Res Commun. 2005; 333(2):328–335. [PubMed: 15961063]

37. Moghimi SM, Hunter AC, Murray JC. Long-circulating and target-specific nanoparticles: theory to practice. Pharmacol Rev. 2001; 53(2):283–318. [PubMed: 11356986]

38. Zhu S, Hong M, Tang G, Qian L, Lin J, Jiang Y, Pei Y. Partly PEGylated polyamidoamine dendrimer for tumor-selective targeting of doxorubicin: the effects of PEGylation degree and drug conjugation style. Biomaterials. 2010; 31(6):1360–1371. [PubMed: 19883938]

39. Lim SM, Kim TH, Jiang HH, Park CW, Lee S, Chen X, Lee KC. Improved biological half-life and anti-tumor activity of TNF-related apoptosis-inducing ligand (TRAIL) using PEG-exposed nanoparticles. Biomaterials. 2011; 32(13):3538–3546. [PubMed: 21306770]

40. Fang YP, Wu PC, Huang YB, Tzeng CC, Chen YL, Hung YH, Tsai MJ, Tsai YH. Modification of polyethylene glycol onto solid lipid nanoparticles encapsulating a novel chemotherapeutic agent (PK-L4) to enhance solubility for injection delivery. Int J Nanomedicine. 2012; 7:4995–5005. [PubMed: 23055719]

41. Chintharlapalli S, Papineni S, Safe S. 1,1-bis(3'-indolyl)-1-(p-substitutedphenyl)methanes inhibit growth, induce apoptosis, and decrease the androgen receptor in LNCaP prostate cancer cells through peroxisome proliferator-activated receptor gamma-independent pathways. Mol Pharmacol. 2007; 71(2):558–569. [PubMed: 17093136]

42. Chintharlapalli S, Papineni S, Baek SJ, Liu S, Safe S. 1,1-Bis(3'-indolyl)-1-(p-substitutedphenyl) methanes are peroxisome proliferator-activated receptor gamma agonists but decrease HCT-116 colon cancer cell survival through receptor-independent activation of early growth response-1 and nonsteroidal anti-inflammatory drug-activated gene-1. Mol Pharmacol. 2005; 68(6):1782–1792. [PubMed: 16155208]

43. Inamoto T, Papineni S, Chintharlapalli S, Cho SD, Safe S, Kamat AM. 1,1-Bis(3'-indolyl)-1-(p-chlorophenyl)methane activates the orphan nuclear receptor Nurr1 and inhibits bladder cancer growth. Mol Cancer Ther. 2008; 7(12):3825–3833. [PubMed: 19074857]

44. Zeng H, Qin L, Zhao D, Tan X, Manseau EJ, Van Hoang M, Senger DR, Brown LF, Nagy JA, Dvorak HF. Orphan nuclear receptor TR3/Nur77 regulates VEGF-A-induced angiogenesis through its transcriptional activity. J Exp Med. 2006; 203(3):719–729. [PubMed: 16520388]

45. Zhao D Fau - Desai S, Desai S Fau - Zeng H, Zeng H. VEGF stimulates PKD-mediated CREB-dependent orphan nuclear receptor Nurr1 expression: role in VEGF-induced angiogenesis. (1097-0215 (Electronic)).

46. Wu Ht Fau - Lin S-H, Lin Sh Fau - Chen Y-H, Chen YH. Inhibition of cell proliferation and in vitro markers of angiogenesis by indole-3-carbinol, a major indole metabolite present in cruciferous vegetables. (0021-8561 (Print)).

47. Chang X, Tou JC, Hong C, Kim HA, Riby JE, Firestone GL, Bjeldanes LF. 3,3'-Diindolylmethane inhibits angiogenesis and the growth of transplantable human breast carcinoma in athymic mice. Carcinogenesis. 2005; 26(4):771–778. [PubMed: 15661811]

48. Yamada S, Bu X-Y, Khankaldyyan V, Gonzales-Gomez I, McComb JG, Laug WE. Effect of the Angiogenesis Inhibitor Cilengitide (Emd 121974) on Glioblastoma Growth in Nude Mice. Neurosurgery. 2006; 59(6)

49. Riby JE, Firestone GL, Bjeldanes LF. 3,3'-diindolylmethane reduces levels of HIF-1alpha and HIF-1 activity in hypoxic cultured human cancer cells. Biochem Pharmacol. 2008; 75(9):1858–1867. [PubMed: 18329003]

50. Mohan HM, Aherne CM, Rogers AC, Baird AW, Winter DC, Murphy EP. Molecular pathways: the role of NR4A orphan nuclear receptors in cancer. Clin Cancer Res. 2012; 18(12):3223–3228. [PubMed: 22566377]

Nanoparticels conjugated with 6His-PEG_{2000}-CREKA through DOGS-Ni-NTA for targeting tumor vasculature (PCNCs-D) by (i) intravenous administration binds to the (ii) clotted plasma proteins on tumor blood vessels and (iii) release the payload. In-Vivo Imaging of (A) tumor bearing mouse with (B) PCNCs-Di targeting reveals tumor vasculature and 30–60 fold enhanced delivery of payload carried by nanoparticle compare to non-targeted nanoparticle (C) NCs-Di.

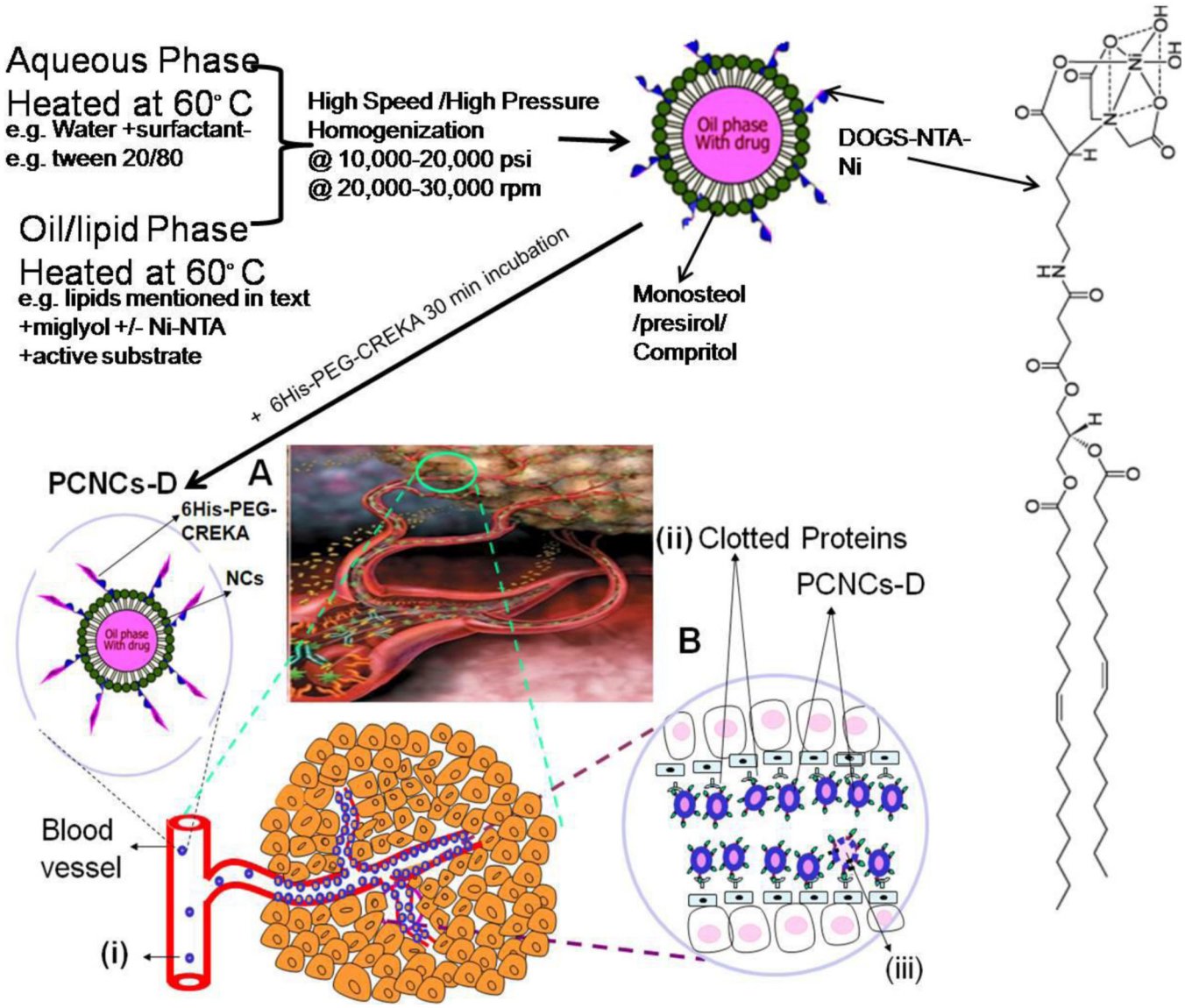

Figure 1.

Schematic diagram of Preparation of NCs and PCNCs with Proposed model for tumor blood vessel targeted CREKA peptide coated NCs system. **A)** Tumor infiltrated with blood vessels; i) administration of targeted PCNCs-D by i.v; **B)** Expanded view of PCNCs-D targeting/accumulation at tumor blood vessels; ii) clotted plasma proteins on tumor blood vessels; and iii) NCs binding to tumor blood vessel following penetration of NCs by enhanced permeation and retention effect (EPR) effect. YKA (nonspecific peptide) coated NCs unable to attach to plasma clot in tumor blood vessels.

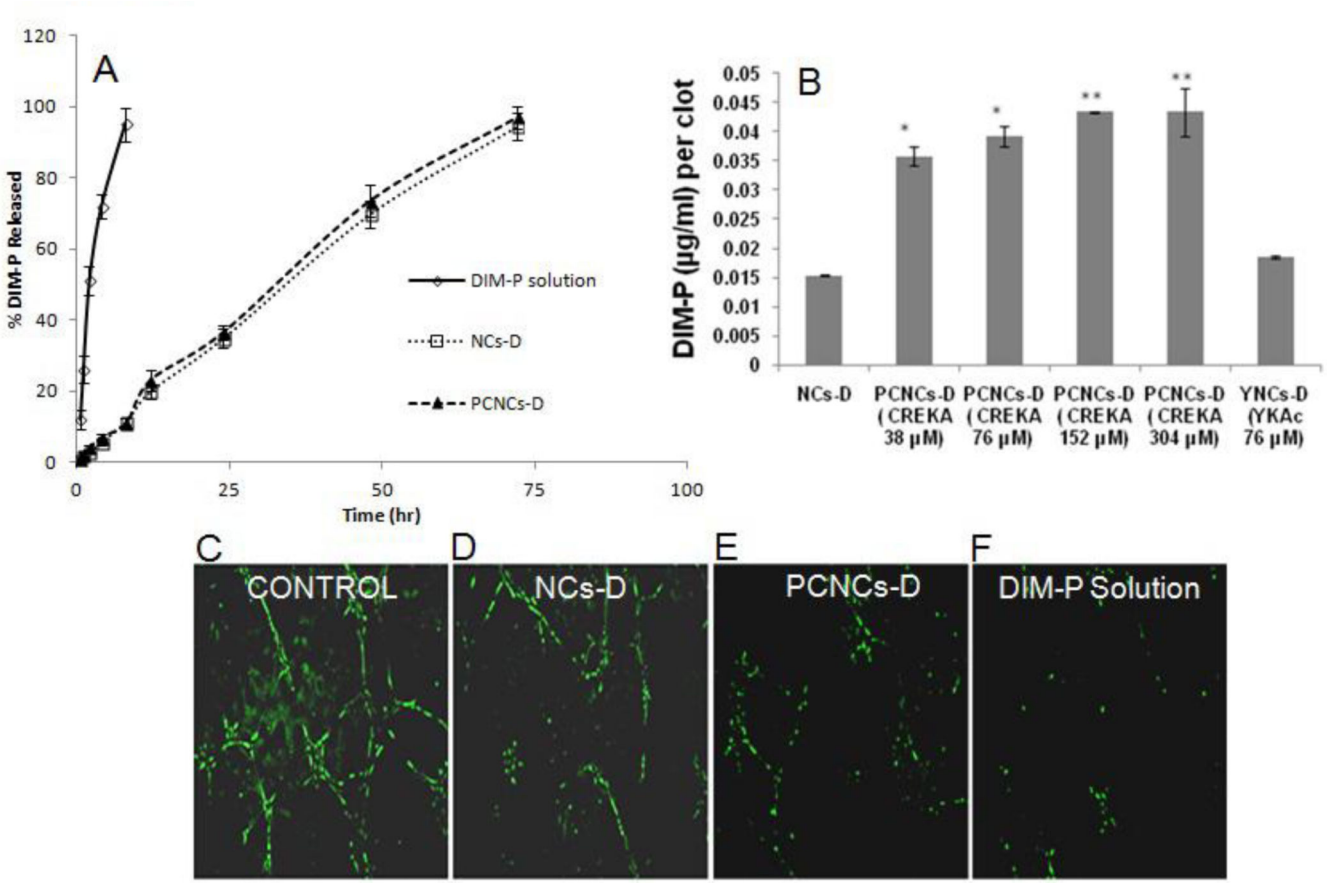

Figure 2.

In-vitro analysis of NCs and PCNCs. **A)** In-Vitro Release Study of DIM-P from NCs-D, PCNCs-D and DIM-P Solution. **B)** Clot binding analysis of NCs-D and PCNCs-D (at different concentration of peptide attached) binding to clotted plasma proteins, (*$p<0.05$, **$p<0.001$). HUVEC cells tube formation after incubation for 6 hr. HUVEC cells were incubated with **C**-Control, **D**-NCs-D, **E**-PCNCs-D and **F**-DIM-P solution on polymerized Matrigel at 37°C. After 6 h, tube formation by PECAM-1(green) endothelial cells was photographed and the capillary tube branch point formation were quantified (n = 3).

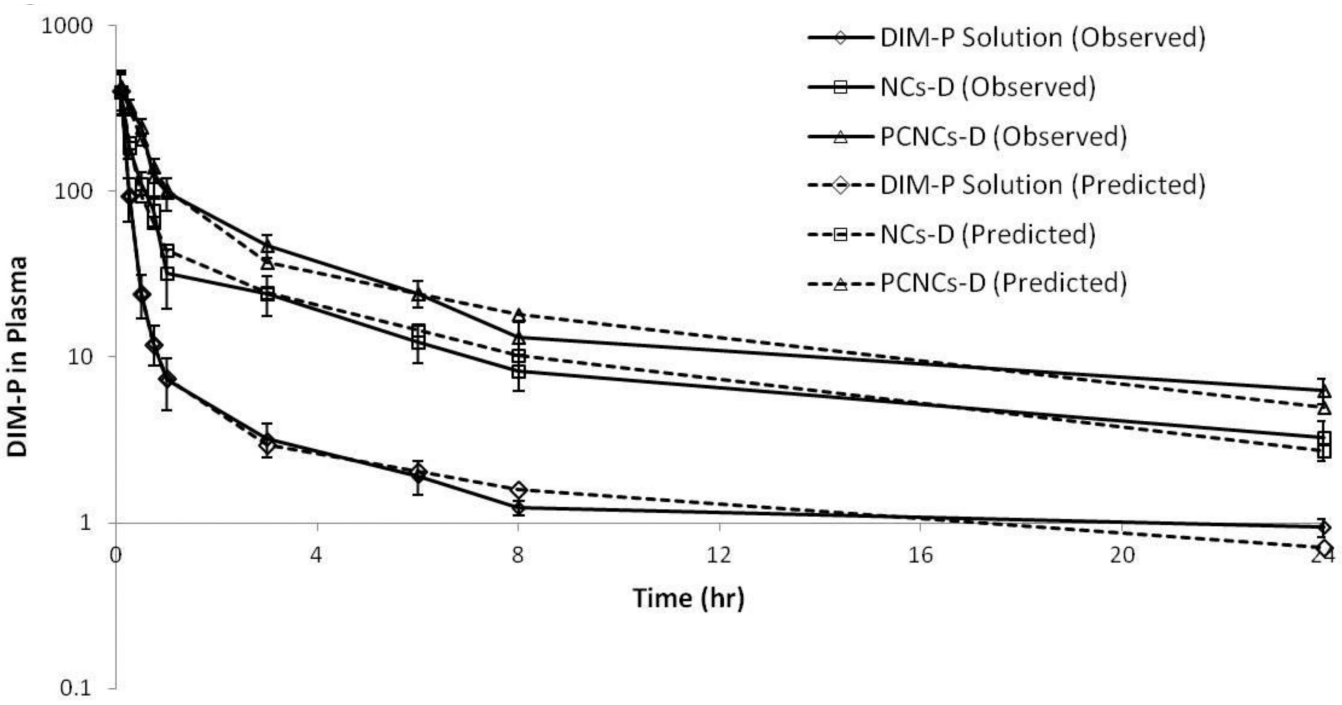

Figure 3.

Plasma Profile of DIM-P in mice following DIM-P Solution, NCs-D, PCNCs-D at 5 mg/kg Intravenous administration.

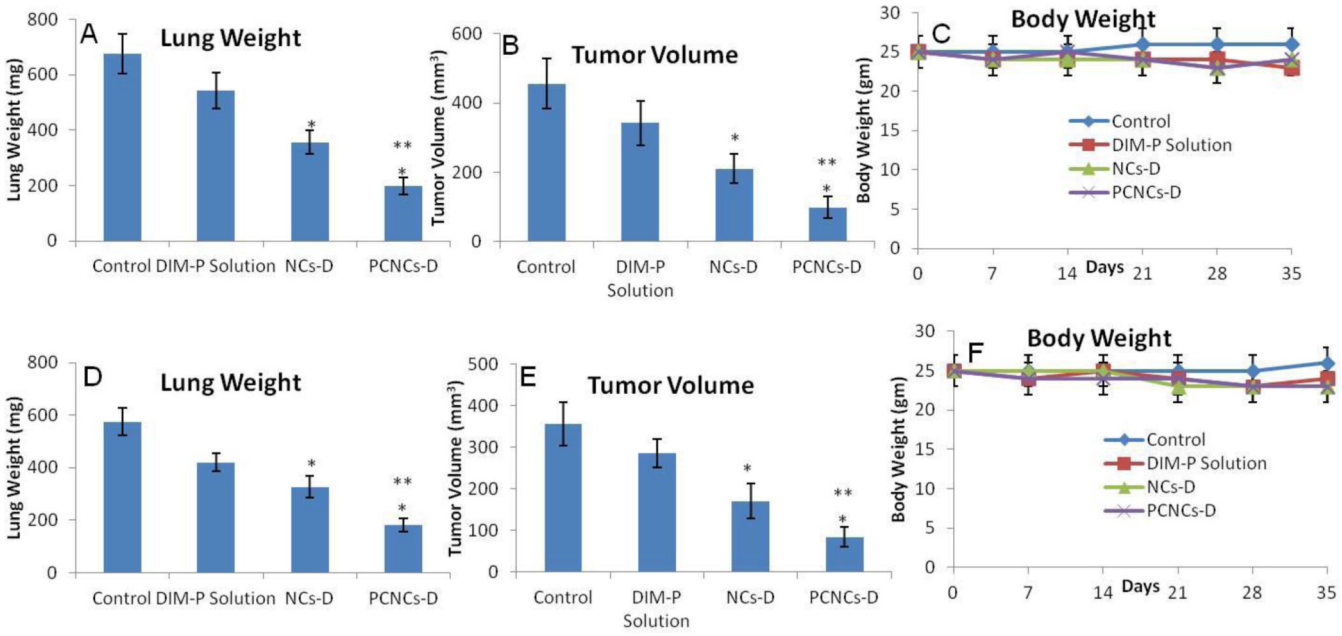

Figure 4.

Effects of NCs-D and PCNCs-D on orthotopic A549 lung tumor weight **(A)**; tumor volume **(B)**; mice body weight **(C)** as well as on metastatic H1650 lung tumor weight **(D)**; tumor volume **(E)**; mice body weight **(F)**. Lung weights and tumor volumes were determined for measurement of therapeutic activity of the treatments. One-way ANOVA followed by post Tukey test was used for statistical analysis. $P < 0.05$ (*, significantly different from untreated controls; **, significantly different from NCs-D treatments). Data presented are means ± SD (n=8).

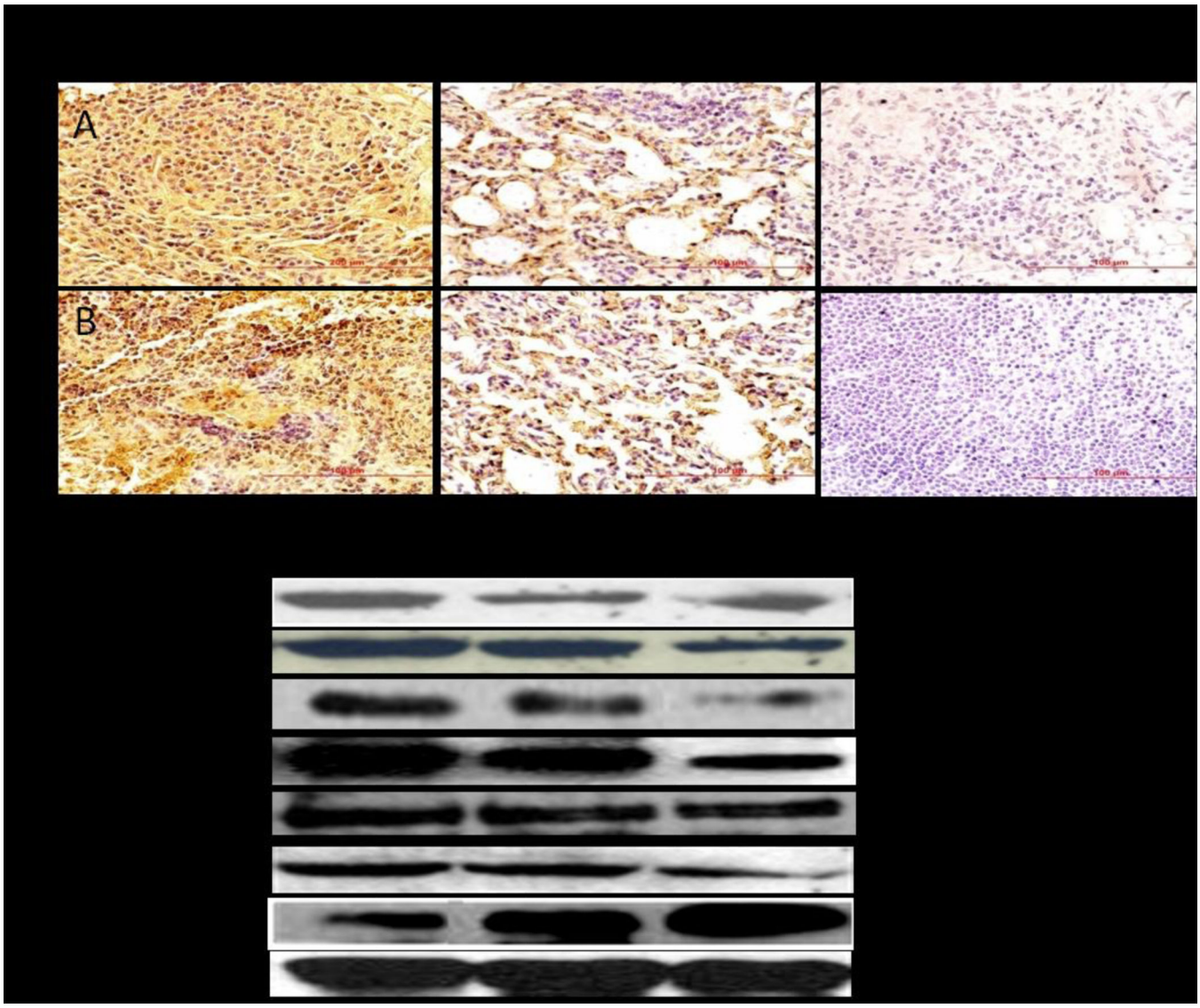

Figure 5.

Immunohistochemical staining of lung tumor tissues for VEGF **(A)** and CD31 **(B)**. Percentages of VEGF and CD31 positive cells were quantitated by counting 100 cells from 6 random microscopic fields. Data were expressed as mean+SD (N=6). Oneway ANOVA followed by post Tukey test was used for statistical analysis to compare control and treated groups. Original magnification ×40 (Micron bar = 100 μm). **(C)** Expression of VEGF, SP1, SP3, HIF-α, HSP-27, MMP-9, and Erk2 proteins in tumor lysates by western blotting. β-actin protein acts as a loading control. Similar results were observed in triplicate experiments. Protein expression levels (relative to β-actin) were determined.

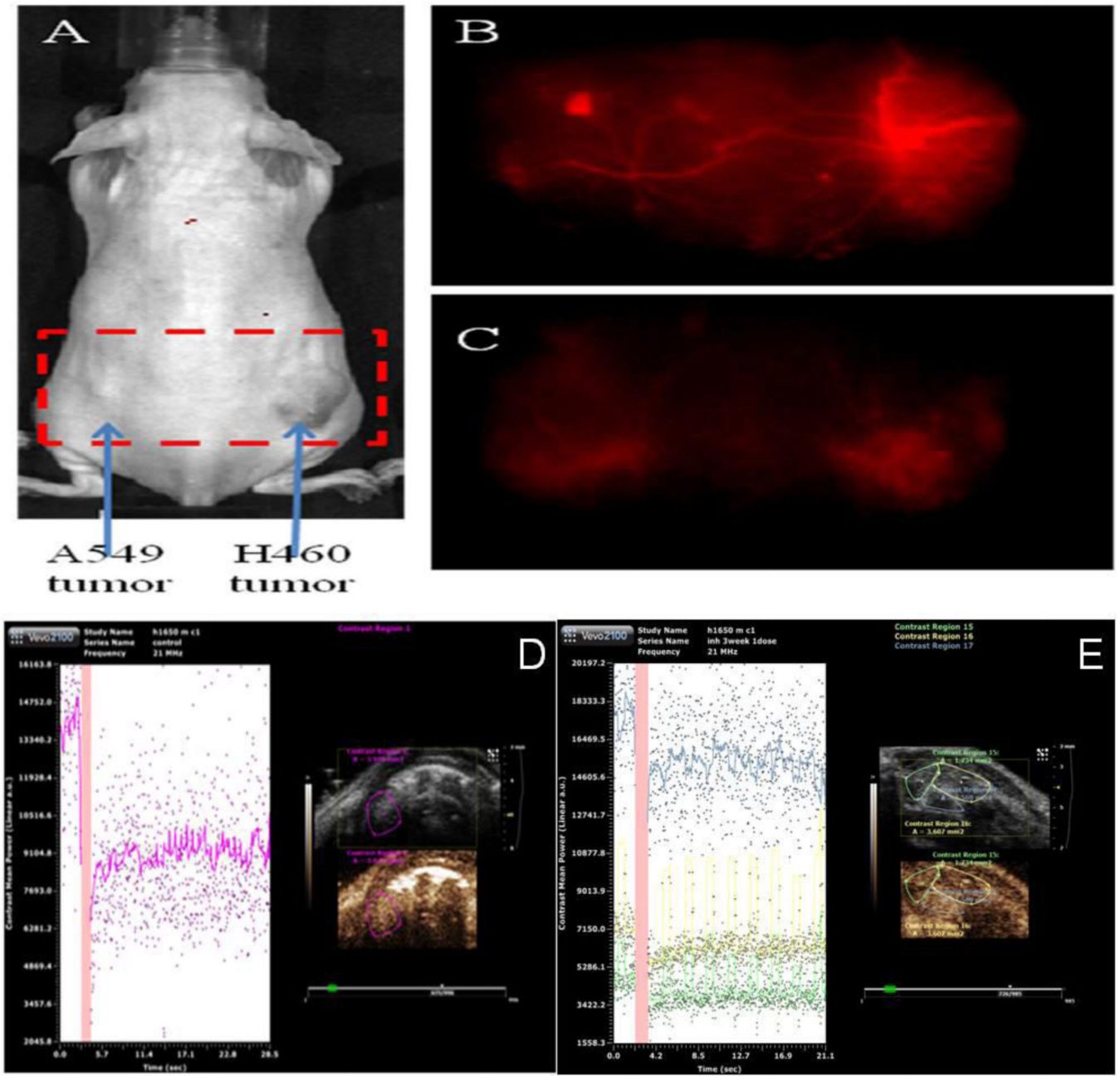

Figure 6.

In-Vivo Imaging. **A)** A549 and H460 lung cancer cell tumor bearing mouse in in-vivo imaging system and Spectrally Unmixed Image of Vasculature with, **B)** PCNCs-Di targeting vasculature and **C)** NCs-Di. Micro-ultrasound is a real-time modality, molecular imaging and quantification of angiogenesis using the microbubbles conjugated to ligands targeting VEGFR2 Control tumor bearing mice **D)** No treatment & **E)** PCNCs-D.